Contemporary Engineering Sciences, Vol. 11, 2018, no. 59, 2911 - 2921
HIKARI Ltd, www.m-hikari.com
https://doi.org/10.12988/ces.2018.86297

Electropulsing Effects on Mechanical and Metallurgical Behavior of AISI-SAE 4140 Steel

Carlos Montilla M.

Mechanical Technology Program
Universidad Tecnológica de Pereira, Vereda La Julita
Pereira, Risaralda, Colombia

Hernán A. González R.

Department of Mechanical Engineering (EPSEVG)
GAECE Research Group
Universitat Politècnica de Catalunya, Av. de Víctor Balaguer
Vilanova i la Geltrù, Barcelona, Spain

Oscar Fabián Higuera C.

Mechanical Engineering Program
CONFORMAT Research Group
Universidad del Atlántico, Carrera 30 N° 8 - 49
Puerto Colombia, Atlántico, Colombia

Valentina Kallewaard E.

Mechanical Engineering Faculty
Universidad Tecnológica de Pereira, Vereda La Julita
Pereira, Risaralda, Colombia

Antonio Sánchez E.

Department of Mechanical and Metallurgical Engineering
Pontificia Universidad Católica de Chile, Av. Vicuña Mackenna 4860
Región Metropolitana, Chile

Abstract

The electroplasticity phenomenon (EP) produces changes in the mechanical properties of a metal, due to the simultaneous application of mechanical stresses of compression, bending, etc., and high instantaneous current pulses. The changes produced on the plastic deformation rate by the EP are due to thermal effects (such as Joule effect) and other effects associated to the electric and magnetic fields. There are only a few studies that consider, as this paper does, the effects of electropulsing effect on tensile test processes in which the electron flow is esteemed as the main reason. In this paper, the results of a research on tensile test on specimen of AISI-SAE 4140, assisted by high-current-density electric pulses are presented. The aim is to evaluate the effect of these pulses on the microstructure and mechanical properties of metallic materials. The phase transformations and microstructural changes in the metallic specimens exposed to EP were analysed using Scanning Electron Microscopy (SEM), Diffraction Ray X (DRX) and Differential Scanning Calorimetry (DSC). Preliminary results show there are some differences in the material behaviour, between the specimens tensile tested with and without EP, such as: decreases values of yield and ultimate strength and XRD analyses attests to a slight displacement and intensity reduction of diffraction. Moreover, the application of current density in the order of 2.18 A/mm² is enough to produce changes in mechanical and metallographic properties of AISI/SAE 4140.

Keywords: Electropulsing, Joule Effect, Tensile Test, Current density

1 Introduction

Electroplasticity Phenomenon (EP) consists in the change of mechanical properties of a metal, due to the application of simultaneous mechanical stresses such as compressive, tensile, flexible as well as instant current pulses [16]. The variation of the strain rate after EP (by pulses or continuous) seems to be explained in terms of thermal effects of Joule heating and the other electrical and magnetic fields. In respect to metal processing, Molostkii and Fleurov [10] reported the following effects of high-density electric current pulses: Stress reduction during processing, fragility decrease, improvement of surface finishing, variation of values for tensile strength and strain, microstructure changes. The study of the aforementioned effects is known as Electrical Assisted Forming (EAF), one of the first published compilations was presented by Salandro et al. [12]. EAF processing relies on the electroplastic effect, where thermal (in micro and macro scale) influences improve deformability of a metallic material [12]. At atomic level, Spitsyn y Troitskii [15] found that external current pulses generate changes on resistivity of metallographic defects such as boundary grain, dislocations and inclusions; promoting dislocation mobility and modification of mechanical behaviour of material. EP during tensile testing has been studied by Magargee et al. [9], Mai et al. [8], Liu et al. [7] y Jae et al. [5]. These researches were performed with testing conditions (temperature, stress

rate, current density) that allow the occurrence of Joule effect [5]. However, those studies neglected the visualization of non-thermal effects from electrical and magnetic fields, and only a few works of EP during tensile test have focused on these thermal effects (Troitskii et al. [18] and Kukudzhanov et al. [6]). Along these lines, the motivation behind this work is to evaluate the occurrence of significant changes of stress-strain curves of AISI-SAE 4140, with a combination of factors (plastic deformation rates, frequency and width of electric pulses) that leads to a Joule heating reduction.

2 Methodology

The AISI-SAE 4140 HSLA steel used in this study was received in soft tempering conditions. Chemical composition (wt.%) is listed in Table 1.

Table 1: Chemical composition of AISI- SAE 4140

Element	C	Mn	Si	P	S	Cr	Ni	Mo
wt.%	0.42	0.79	0.24	0.018	0.022	1.06	0.11	0.19
Element	Cu	Al	Sn	V	Ti	Nb	Pb	
wt.%	0.13	0.014	0.009	0.003	0.002	0.003	0.001	

The microstructure of the samples was characterized with Scanning Electron Microscopy (SEM) and Energy Dispersive X Ray Spectroscopy using a ZEISS EVO/MA10 scanning electron microscope at 20 kV accelerate voltage. Additionally, the residual stresses, crystallographic orientation and lattice parameters of the samples were obtained by X-ray diffraction (XRD), Co-Kα radiation (λ = 1.788965 Å) by means of Phillips X'pert Pro Panalytical diffractometer. XRD also determined crystal size resorting to *Scherrer* Equation [4]. Characterization also took into account probable internal stress during electro-pulsing-assisted tensile testing, that could contribute to the diffraction peak broadening. Equation (1) helps to estimate the relation among peak broadening, crystal size and micro-stress [4].

$$\beta^2 = \left(\frac{0{,}94\,\lambda}{D\cos\theta} \right)^2 + \left(4\varepsilon \tan\theta\right)^2 + \beta_0^2 \tag{1}$$

Where β is the broadening of average peak by FWHM (full width at half maximum), λ is X-Ray wavelength, D is average crystallite size, ε is microstrain, θ is Bragg Angle and is βo= 0,03514° is instrumental broadening [4].

XRD estimated residual stress based on pinhole method, which was applied under the following assumptions: isotropic stress (σ), biaxial state of stresses and equivalence of principal stresses in terms of magnitudes. Thus, leading to following equation [4]:

$$\sigma = \left(\frac{E}{2*\vartheta}\right) * \left(\frac{a_0 - a}{a_0}\right) \quad (2)$$

Where E is Young's modulus (200 GPa), ϑ is Poisson's ratio (0,3) and a_0 (2.8637Å) and a are measurements of lattice parameters of Fe-α (BCC). Values were obtained from literature [2].

2.2. Mechanical Behaviour

Specimens were machined in compliance with ASTM E-8 standard [2], their dimensions are illustrated in Figure 1a. Cross section of gage length is 6.47 mm^2. Tensile testing was performed in *Ibertest* UMIB – 600SW universal testing machine with variation of stress rates, the respective set up is shown in Figure 1b.

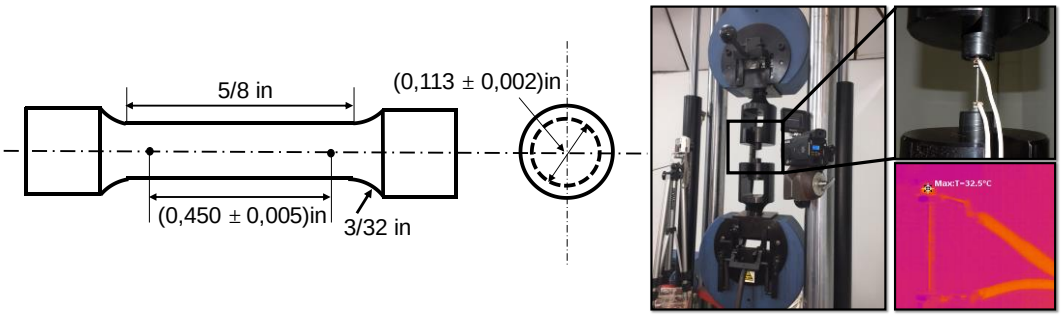

(a) (b)

Figure 1. (a) Dimensions of specimens. (b) Experimental set up of tensile testing.

In order to reduce Joule heating, the tensile testing was assisted by electric pulses with frequency of 300Hz and width of 200μs. That is to say, room temperature was in order of 29.0ºC, while specimens reached temperatures in the order of 32.0 ºC (According to thermal image of Figure 1b. Aforementioned values of frequency and width could be guaranteed thanks to design of control and power electronics of generators [13]. Table 2 summarizes parameters of tensile test including data of reference samples without affectation by electric pulses.

Table 2. Mechanical and electrical parameters during tensile testing.

Condition	Stress rate (N/s)	Frequency (Hz)	Width (μs)	Current density (A/mm²)
1	2	0	0	-----
2	6	0	0	-----
3	10	0	0	-----
4	2	300	200	2.18
5	6	300	200	2.18
6	10	300	200	2.18
7	75	300	200	4.20
8	3000	300	200	4.20
9	30000	300	200	4.20

3 Results

3.1 Mechanical Characterization

The analysis of mechanical resistance presented herein considered the study of three properties: Yield and Ultimate Tensile Strength and % Elongation (Table 3), and the corresponding apparent stress strain curves are illustrated in Figure 2. In this study, yield strength is assumed as the value of proportionality limit at the beginning of yielding.

Firstly, the comparative study focused on tensile testing cases subjected to lower stress rates regardless of the presence of electric-pulse assistance; that is to say, the first six cases. Overall, lower mechanical resistance was reported for specimens with pulse train, which can be clearly seen with the comparison of Figures 2a and 2b. It is worth mentioning, these variations of mechanical resistance were achieved with lower current density that the one applied in previous studies [9, 8, 7, 5].

Next, aiming to a better understanding of the affectation of train pulse assistance by both stress rate and current density, complimentary tests increased current density from 2.18 to 4.20 A/mm² with higher stress rates (75, 3000 and 30000 N/s). After comparing the corresponding data from Table 3 and Figure 2b and 2c, a tendency of recovery on mechanical resistance can be attested. However, such a recovery did not match the values obtained for samples without train pulses. Finally, data from Table 3 shows that electric pulse did not affect % elongation significantly.

Table 3. Mechanical properties studied during tensile testing

Conditions	Yield strength (MPa)	Ultimate strength (MPa)	Elongation %
1	726	953	13.8
2	819	1098	15.4
3	707	915	11.9
4	627	882	12.6
5	540	749*	12.6
6	535	776	12.0
7	530	755	13.2
8	602	856	11.1
9	688	925	13.1

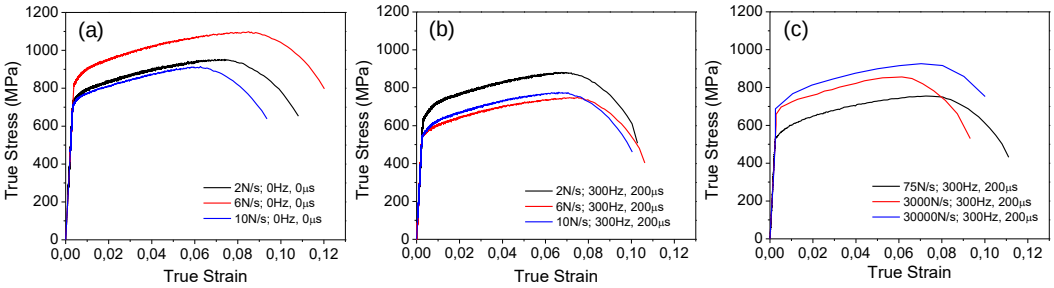

Figure 2. Mechanical behaviour of AISI SAE 4140 Steel. (a) without pulses, (b) and (c) with pulses.

3.2 Microstructural characterization

To a great extent, after being subjected to tensile testing, specimens preserved a martensite/bainite microstructure; the same microstructure corresponding to quenched and tempered as-received AISI-SAE 4140. However, the presence of micro-components (annealed martensite, inferior and superior bainite), can be seen. Specimens subjected to 75 N/s (Figure 3a) y 3000 N/s (Figure 3b) exhibited a more stable behaviour in comparison to samples subjected to 30000 N/s (Figure 3c) with a more stressed microstructure. The latter specimens reported a greater area of inferior bainite as compared to 75 and 3000 N/s cases. For a better understanding of the presence of phases and micro components, XRD analysis will be given in next section.

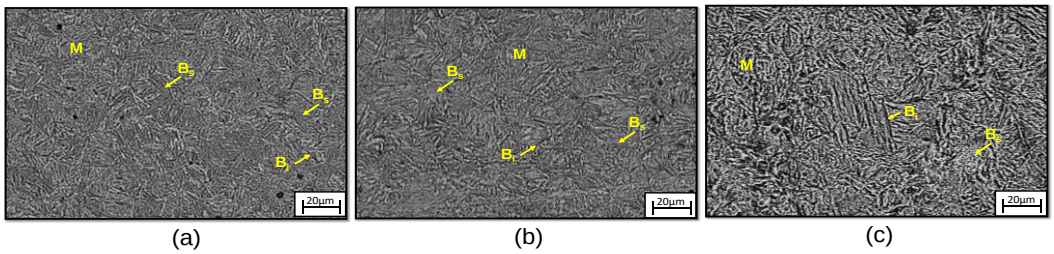

Figure 3. Microstructural behaviour of AISI 4140 subjected to (a) 75 N/s, 300 Hz, 200 µs, (b) 3000 N/s, 300 Hz, 200 µs and (c) 30000 N/s, 300 Hz, 200 µs. Annealed martensite (M), inferior bainite (B_i) and superior bainita (B_s).

Figure 4 illustrates XRD corresponding to specimens after tensile testing with and without electric pulses with conditions listed on Table 2. Figure 4a reports a behavior similar to that of the typical machinery steel whose microstructure has martensite, as in the case of as-received ASI 4140 (quenched at 850°C and tempered at 500°C). Such a tempering treatment triggered loss of tetragonality of martensite as well as the formation and recrystalization of cementite due to thermal treatment spheroidization. Given the previous explanation, the material is assumed as BCC martensite for the purpose of this study. The values of lattice parameters ***a*** were obtained by means of Equation (3) [16] based on interplanar spacing d_{hkl} from each

diffraction peak. Both sets of data (***a*** and d_{hkl}), that are in strong agreement with models proposed in the literature where chemical compostion of the alloy [3], see Table 4.

$$d_{(hkl)} = \frac{a_0}{\sqrt{(h^2+k^2+l^2)}} \tag{3}$$

Bear in mind that AISI 4140 with 0.42%C, after quenching (as-received condition) presents a martensite with a relation *c/a*≈ 1.0239 according to *c/a*= 1.005+0.045*%C [16]. Subsequently, after tempering, *c/a* relation has a value approximately equal to 1 due to formation of metastable carbides (epsilon carbide $Fe_{2.4}C$ y Hagg Fe_5C_2) during the first stage of tempering. As tempering temperature increases, those carbides will transform into stable carbide Fe_3C [17].
Diffraction patterns of Figure 4b and 4c reports peaks in planes (110) and (200) very similar to those corresponding to BCC martensite.

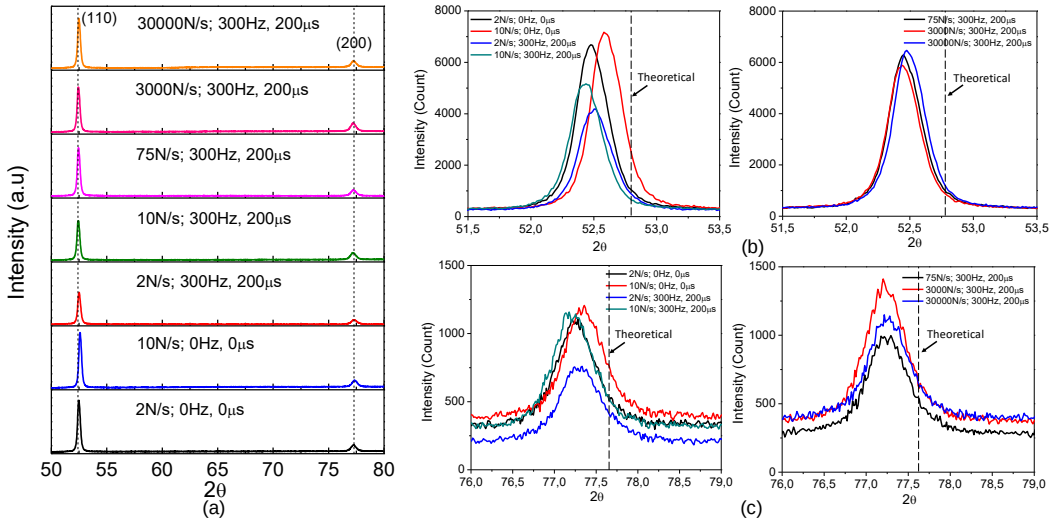

Figure 4. (a) XRD spectra of samples after tensile testing with variation of stress rates, width and frequency of electric pulses. (b) peak (110) and (c) peak (200).

All the peaks (110) and (200) from Figures 4b and 4c present slight displacements in respect to the reference lines, for all the conditions of tensile testing listed in Table 2. The greatest intensity decreases are reported for peaks (110) corresponding to cases assisted by electric pulses with low stress rates (2 and 10 N/s). Such a low intensity could be associated to either the presence of micro-stresses, machining prior to tensile testing, residual stresses due to tempering and quenching or EP effect combined with variation of stress rates [14].

Micro-stresses (σ) data from Table 4 were calculated for both diffraction peaks, more significant changes took places for peak (200). In comparison to peak (110), plane (200) may be less affected by the external effects during previous sample preparation.

Regarding the length of interplanar spacing, the results presented herein are in strong agreement with Bragg law. That is to say, a grain subjected to a non-uniform stress perpendicular to the diffraction planes, will present zones where interplanar spacing d_{hkl} can be either greater or less than d_{0hkl} [4]. According to Figure 4b, this behaviour is considerably more evident for peaks (110), especially for conditions 6, 7 and 8 (10, 75 and 3000 N/s with EP), whose interplanar spacing d_{hkl} are the longest: 2.0247, 2.042 and 2.0247 Å. This behaviour is also corroborated in Figure 4, where diffraction peaks (110) and (200) were displaced to a lower 2θ.

Table 4. XRD Parameters

Conditions from Table 2	**P**eak	2θ (°)	d_{hkl} (Å)	β (°)	D (Å)	ε (GPa)	A (Å)	σ (GPa)
1	(110)	52.4766	2.0233	0.2588	422.155	0.02933	2.8614	0.0243
	(200)	77.2806	1.4325	0.2588	368.9667	0.02051	2.8650	-0.014
3	(110)	52.5806	2.0196	0.2505	440.9415	0.03089	2.8561	0.079
	(200)	77.3586	1.4313	0.2505	396.4276	0.02075	2.8626	0.011
4	(110)	52.5156	2.0219	0.2765	392.8248	0.03535	2.8594	0.045
	(200)	77.3326	1.4317	0.2765	282.2173	0.02433	2.8634	0.003
6	(110)	52.4376	2.0247	0.2733	404.8439	0.03160	2.8633	0.0036
	(200)	77.1766	1.4341	0.2733	231.2475	0.01989	2.8682	-0.047
7	(110)	52.4506	2.0242	0.2611	417.6988	0.02902	2.8627	0.011
	(200)	77.2936	1.4323	0.2611	357.7007	0.02112	2.8646	-0.009
8	(110)	52.4376	2.0247	0.2597	431.709	0.02837	2.8633	0.0036
	(200)	77.2026	1.4337	0.2597	232.4691	0.01810	2.8674	-0.039
9	(110)	52.4766	2.0233	0.2581	421.656	0.02915	2.8614	0.024
	(200)	77.2156	1.4335	0.2581	373.0045	0.01915	2.867	-0.035

4. Conclusions

One study of tensile test on specimen of AISI-SAE 4140, assisted by high-current-density electric pulses has been done.

The effect of electric pulses on the microstructure and mechanical properties of metallic materials show there are some differences in the material behaviour, between the specimens tensile tested with and without EP.
In comparison to conventional tensile testing, the application of electric pulse during this kind of test on AISI 4140 steel, decreases values of yield and ultimate strength, reporting the most significant reductions for the conditions with lower stress rates (2, 6 and 10 N/s). Mechanical characterization did not report significant variation of % elongation.

Results also show that application of current density in the order of 2.18 A/mm² is enough to produce changes in mechanical and metallographic properties of AISI/SAE 4140.

XRD analyses attests to a slight displacement and intensity reduction of diffraction peaks corresponding to samples subjected to low stress rates (2 y 10 N/s), regardless of the presence of electric pulses.

Acknowledgements. The authors want to thanks to Universidad Tecnológica de Pereira, for facilitating the economic resources, facilities and laboratories used in the physical execution of the present study. In addition, this work was also supported by the National Council for Scientific and Technological Development of Chile (Fondecyt Projects 3180006)

References

[1] ASTM E8, Standard Test Method for Tension Testing of Metallic Materials, U.S.A., 2004.

[2] W. Callister Jr., *Fundamentals of Material Science and Engineering*, Ffth edition, John Wiley & Sons, Inc. USA, 2001.

[3] A.H. Cottrell, *Theoretical Structural Metallurgy*, Edward Arnold, 1962.

[4] B.D Culity, *Elements of X-ray Diffraction,* Second edition, Addison Wesley Publishing Company, 1978.

[5] R. Jae-Hun, S.O. Jeong-Jin, H. Sung-Tae, K. Moon-Jo, N.H. Heung and J.T. Roth, The mechanical behavior of 5052-H32 Aluminum Alloys under a Pulsed Electric Current, *International Journal of Plasticity*, **58** (2014), 84–99. https://doi.org/10.1016/j.ijplas.2014.02.002

[6] V.N. Kukudzhanov and A.V. Kolomiets-Romanenko, A Model of Thermoelectroplasticity of Variations in the Mechanical Properties of Metals based on Defect Structure Reorganization under the Action of Pulse Electric Current, *Mechanics of Solids*, **46** (2011), 814–827. https://doi.org/10.3103/s0025654411060021

[7] K. Liu, X. Dong, H. Xie and F. Peng, Effect of Pulse DC Current on the deformation behavior of AZ31B Magnesium Alloy, *Materials Science & Engineering A*, **623** (2015), 97–103. https://doi.org/10.1016/j.msea.2014.11.039

[8] J. Mai, L. Peng, Z. Lin and X. Lai, Experimental Study of Electrical Resistiyity and Flow Stress of Stainless Steel 316L in Electroplastic Deformation, *Material Science and Engineering A*, **528** (2011), 3539-3544.

https://doi.org/10.1016/j.msea.2011.01.058

[9] J. Magargee, F. Morestin and C. Jian, Characterization of Flow Stress for Commercially Pure Titanium subjected to Electrically Assisted Deformation, *Journal of Engineering Materials and Technology*, **135** (2013), 041003-1. https://doi.org/10.1115/1.4024394

[10] M. Molotskii and V. Fleurov, Magnetic Effects in Electroplasticity of Metals, *Physical review B*, **52** (1995), no. 22, 15829-15834. https://doi.org/10.1103/physrevb.52.15829

[11] D.A. Porter and K.E. Easterling, *Phase Transformations in Metals and Alloys*, Springer-Science, Business Media, 1992.

[12] W.A. Salandro, J.J. Jones, C. Bunget, L. Mears and J.T. Roth, *Electrically Assisted Forming. Modeling and Control*, Springer, 2015. https://doi.org/10.1007/978-3-319-08879-2

[13] A.J. Sánchez, H.A. González, C.A. Montilla and V. Kallewaard, Manufacturing Improves when Turning Process is assisted in situ by Short Time Electropulsing, *Journal of Materials Processing Technology*, **222** (2015), 327–334.

[14] A.J. Sánchez, H.A. González, D. Celentano, J. Jorba and J. Cao, Thermomechanical Analysis of an Electrically Assisted Wire Drawing Process, *Journal of Manufacturing Science and Engineering*, **139** (2017), 111017. https://doi.org/10.1115/1.4037798

[15] V. I. Spitsyn and O. A. Troitskii, *Deformación Electroplástica De Metales*. Editorial Nauka, Moscú, 1985.

[16] A.F Sprecher., S.L Mannan and H. Conrad On the mechanisms for the Electroplastic Effect in Metals, *Acta Metall*, **34** (1986), no. 7, 1145-1162. https://doi.org/10.1016/0001-6160(86)90001-5

[17] G. Totten, *Steel Heat Treatment. Metallurgy and Technologies*, Second edition, Taylor & Francis Group, Boca. 2006. https://doi.org/10.1201/nof0849384523

[18] O.A. Troitskii and V.I. Likhtman, The Effect of the Anisotropy of Electron and

Radiation on the Deformation of zinc single crystals in the Brittle State, *Akaciemiya Nauk SSSR*., **147** (1963), no. 4.

Received: July 14, 2018; Published: August 2, 2018